Wayne State University Theses

1-1-2012

The Spliceosomal Protein Prp8 Stabilizes A Compact Conformation Of The U2-U6 Complex

Subasinghe Appuhamilage Lemintha Imali Subasinghe
Wayne State University,

Follow this and additional works at: http://digitalcommons.wayne.edu/oa_theses

THE SPLICEOSOMAL PROTEIN PRP8 STABILIZES A COMPACT CONFORMATION OF THE
U2-U6 COMPLEX

by

S. A. L. IMALI SUBASINGHE

THESIS

Submitted to the Graduate School

of Wayne State University,

Detroit, Michigan

in partial fulfillment of the requirements

for the degree of

MASTER OF SCIENCE

2012

MAJOR: CHEMISTRY (Biochemistry)

Approved by:

_____
Advisor   Date

DEDICATION

To my family

ACKNOWLEDGMENTS

I had amazing, life-lasting experiences at the Wayne State University and in the Rueda Lab. I am very grateful to a number of people for giving me the opportunity to study in this environment and helping me throughout the process.

First and foremost, I would like to express my sincere gratitude to my advisor, Prof. David Rueda, for continuous support during my studies and research. His patience, motivation, enthusiasm, immense knowledge and admiration of the lab work and my project have been instrumental in my development. I am grateful for his systematic guidance and diligent effort to train me to be an independent scientist and a critical thinker. I cannot imagine learning under a more capable and caring advisor.

I'm also thankful to my thesis committee, Prof. Christine Chow and Prof. Arthur Suits for their encouragement and insights on my research. Professors Andrew Feig, Ashok S. Bhagwat, John SantaLucia Jr., Mary Kay Pflum, Mary T. Rodgers and Tamara L. Hendrickson were extremely supportive during my coursework. I also wish to thank Dr. Amanda Solem for training me when I first joined the lab and Dr. Alfonso Brenlla for technical support with the single-molecule setup.

There are numerous other people that deserve recognition and acknowledgment in the development of this document. My past and present labmates, including Chandani, Hansini, Bishnu, May, Eric, Pramodha, Rajan, Krishanthi, and Rui, have always provided me with stimulating discussions and also light-hearted moments during the last two years. I am also thankful for a supportive administrative departmental staff including Melissa, Debbie, Diane, Bernadette and Nestor. I have also learned a lot from

TABLE OF CONTENTS

LIST OF FIGURES

CHAPTER 1: Introduction

1.1: Pre-mRNA splicing is carried out by the spliceosome. Pre-mRNA splicing is the removal of non-coding sequences (introns) and the ligation of coding sequences (exons) via two transesterification reactions during the maturation to mRNA [1] (Fig. 1). During the first transesterification reaction, the 2'-hydroxyl group of the branch site adenosine attacks the 5' splice site, and during the second transesterification reaction the free 3' hydroxyl group of the 5' exon attacks the 3' splice site, ligating the two exons and releasing the intron as a lariat structure [1]. Pre-mRNA splicing is carried out by a multi mega-Dalton RNA-protein complex called the spliceosome [1]. Two different types of spliceosomes coexist in many eukaryotes; the more common U2-dependent spliceosome, which is the focus of this study, and the less abundant U12-dependent spliceosome [1]. The U2-dependent spliceosome consists of five snRNAs (U1, U2, U4, U5 and U6) and more than seventy proteins in yeast and about one-hundred proteins in humans [1-3].

The structure and composition of the spliceosome change throughout the splicing reaction, making the spliceosome one of the most complex biological machines [4]. Splicing begins with the recognition of the 5' splice site and branch site by U1 and U2 snRNAs, respectively, to form the pre-spliceosome (**Fig. 2**). The tri-snRNP complex, U4/U6·U5, is then recruited to the pre-spliceosome generating the penta-snRNP structure called the pre-catalytic spliceosome (complex B). The DExD/H-box family helicases, Prp28 and Brr2, then cause a large-scale structural rearrangement in the spliceosome [1]. As a result, the U4/U6 duplex is unwound and the U6 snRNA forms

base-pair interactions with U2. The U1/5' splice-site interaction is also disrupted and replaced with a U6/5' splice-site interaction, forming the activated spliceosome, (B^{act}) [1]. B^{act} is then converted to the catalytically activated spliceosome (B^*) in a reaction mediated by the protein Prp2 [1]. After the first transesterification reaction, B^* forms the complex C, which performs the second transesterification reaction to ligate the two exons and release the branched intron (**Fig.2**). The snRNAs can then be re-used in another splicing reaction.
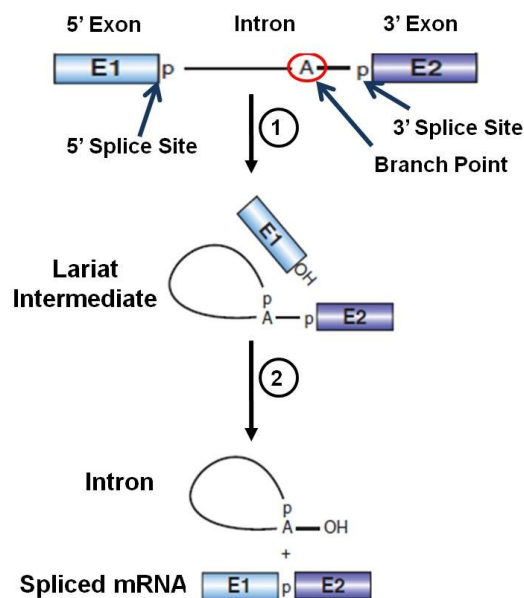
Figure 1: Two transesterification reactions occur during splicing [1]. First, the 2'-hydroxyl group of branch site adenosine (circled in red) attacks the 5' splice site resulting a free 3'-OH of 5' exon and a branched intron attached to the 3' exon. Second, 3'-OH of the 5' exon attacks the 3' exon, ligating the two exons and removing the lariat intron.

1.2: Only a few components are present at the active site of the spliceosome.

Despite the complexity, only a few components are present in the active site of the spliceosome [5]. These include U2 and U6 snRNAs, as well as the U5 snRNP protein, Prp8 [5-7]. In the active spliceosome, U2 and U6 form extensive base pairs with each other (**Fig. 3**) and the branch site and the 5' splice site, respectively. High sequence
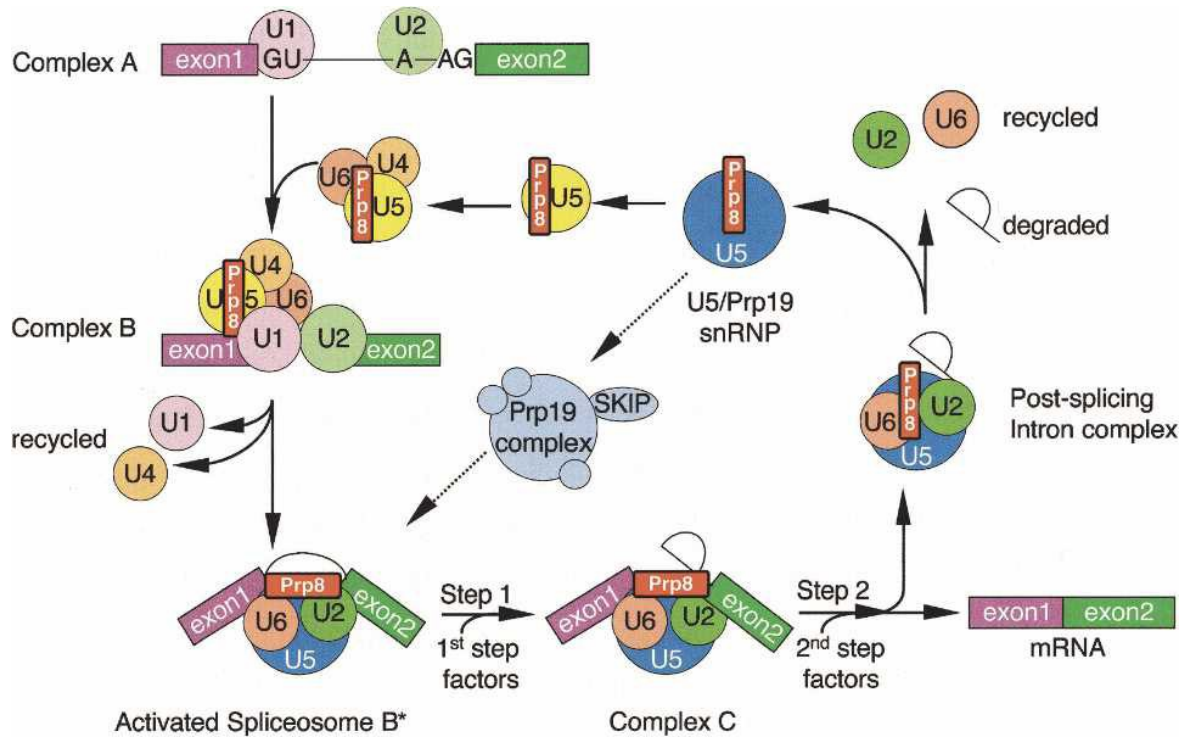
Figure 2: Assembly and the catalysis of the spliceosome. Exons and introns are shown in boxes and black lines respectively. Circles represent the five snRNAs. The U5 snRNP protein, Prp8, enters the cycle at complex B and remains attached until the end [8].
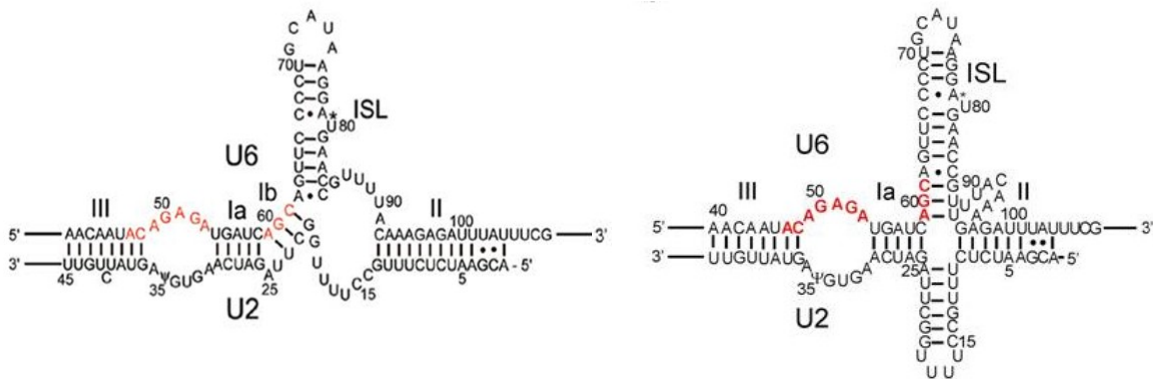
Figure 3: Alternative secondary structures adopted by the U2-U6 complex. The three-helix junction proposed by the Guthrie lab suggests that the invariant AGC triad (red) of U6 form intermolecular base pairs with U2 (Left) [9], while the four-helix junction proposed by the Butcher lab suggests AGC triad form intramolecular base pairs extending the U6 ISL (Right) [10].

conservation, structural similarity to the group II intron domain V (DV) [11], and genetic

studies have lead to the proposal that U6 plays a catalytic role in pre-mRNA splicing.

Group II introns are self-splicing ribozymes that are present in certain bacteria [12], fungi and plants [13]. Both DV of group II introns and U6 snRNA contain an invariant AGC triad, GNRA-type loop, and a one- or two-nucleotide bulge in almost identical locations [5]. In U6 snRNA, the AGC triad is found to be important in both catalytic steps of splicing [14, 15]. The GNRA-type loop in the group II intron forms a tertiary interaction to properly position DV in the active site [16]. It is believed that the GNRA-type loop in the spliceosome is also involved in tertiary interactions to facilitate splicing [5]. Crystal structure and phosphorothioate substitution studies show that both bulge regions of DV and U6 ISL (A376-C377 of group II intron and U80 of U6 ISL) bind a metal ion that has been shown to be important for the catalysis [17-21]. These studies suggest that both group II introns and the spliceosome may have evolved from a common ancestor, and hence the spliceosome is a ribozyme [20, 22].

1.3: The U2-U6 complex adopts multiple conformations. The structure adopted by U2-U6 has been a matter of debate for the past few years. Yeast genetic studies from the Guthrie lab [9] suggest that the U6 AGC triad forms intermolecular base pairs with U2, and therefore, the U2-U6 complex adopts a three-helix junction (Fig. 3). On the other hand, mammalian genetic studies from the Manley lab [23] and early NMR studies carried out on a shorter construct from the Butcher lab suggest that the invariant AGC triad forms intramolecular base pairs, adopting a four-helix junction [10] (Fig. 3), while later NMR studies carried out on a longer U2-U6 construct suggest a three-helix junction [24].

Previous smFRET studies carried out on a minimal U2-U6 construct from our lab showed that U2-U6 adopts at least three dynamic conformations with distinct FRET

states (~0.2, ~0.4 and ~0.6) [25]. The relative populations of the three FRET states revealed by smFRET are dependent on Mg^{2+} concentration [25]. With increasing Mg^{2+} concentration, the low FRET state populations are increased, while with decreasing Mg^{2+} concentrations, the high FRET states populations are increased. Furthermore, the ACAGAGA sequence, AGC triad, and U80 of U6 have been hypothesized to form base-triple interactions that are proposed to stabilize the high FRET state (**Fig. 4**) [26]. It is hypothesized that when Mg^{2+} is bound, U80 is stacked into the helix [24], and therefore it can no longer participate in the base-triple formation, and hence, there is an increase in the population of the low FRET state. In contrast, when Mg^{2+} is not bound, U80 is flipped out from the U6 ISL, and the high FRET state is favored. According to this model, when Mg^{2+} is bound, the distance between the U6 ISL and the ACAGAGA sequence is increased, which in turn increase the distance between the bound metal ion and the 5' splice site. Therefore, it is believed that with a constant supply of Mg^{2+} *in vivo*, protein factors may adjust the relative stability of the U2-U6 dynamic conformations to achieve efficient splicing [5, 24, 25].

1.4: The spliceosomal protein, Prp8, may play an important role in splicing catalysis. The idea that the spliceosome is a ribozyme has been challenged with the identification of the U5 snRNP protein, Prp8, which is one of the largest (2413 and 2335 residues in yeast and human, respectively) [27] and well-conserved proteins found in the nucleus [28-30]. Of all the spliceosomal proteins, Prp8 is the only protein that extensively cross-links to the 5' and 3' splice sites of the substrate pre-mRNA, U5 and U6 snRNA [31, 32], indicating a catalytic or structural role of Prp8 in splicing [33].

Studies have shown that Prp8 has several domains, such as a nuclear-localization

domain (NLS), RNA recognition motif (RRM), Jab1/MPN domain, and an RNase H-like
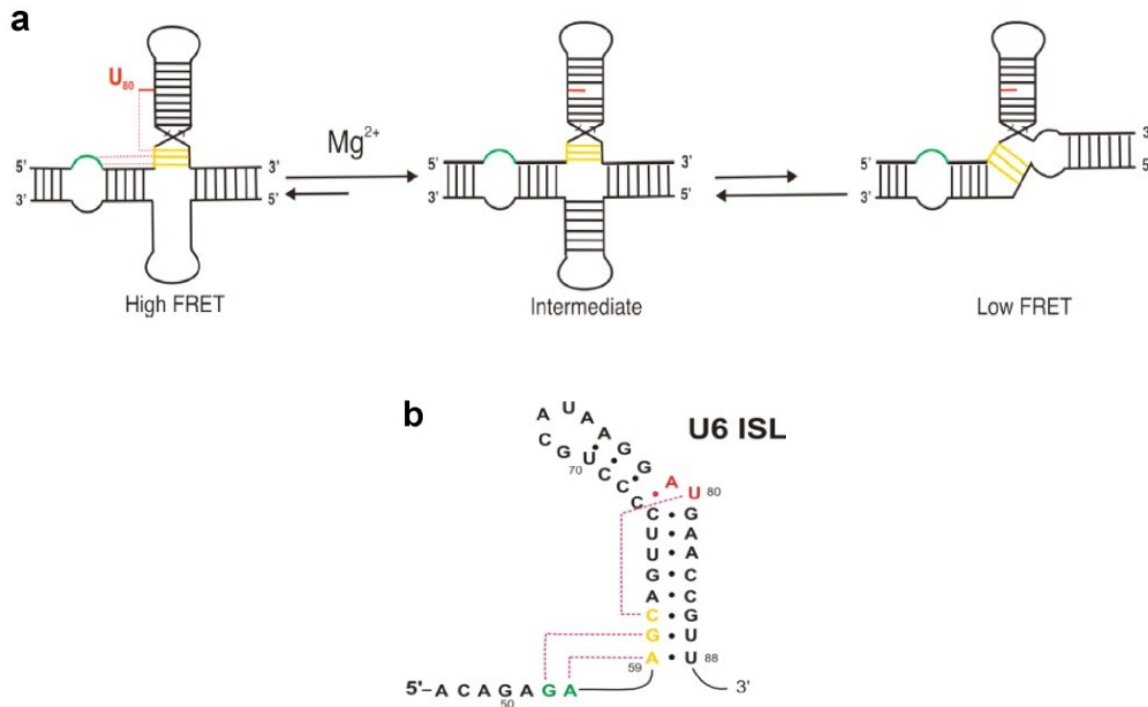
Figure 4: The proposed U2-U6 folding pathway. **(A)** Base-triples are proposed to stabilize the high FRET state. When Mg2+ is bound, the conformation is changed and U2-U6 goes to the low FRET state via an intermediate. **(B)** The proposed base-triple interactions between ACAGAGA sequence, AGC triad and U80 [26].

domain [6, 29, 30]. Within the past few years, three groups have resolved the X-ray

crystal structure of a ~250 amino-acid fragment near the C-terminus of yeast and

human Prp8 [27, 30, 34]. Although there are slight conformational differences between

yeast and human structures, all three groups revealed the presence of an RNase H

domain, which consists of two parts, the N-terminal subdomain with an RNase H fold

and a C-terminal subdomain consisting of five alpha helices [6]. The human RNase H

domain has a characteristic five parallel/antiparallel beta strands buttressed by two

alpha helices [30] (**Fig. 5**). In addition to the aforementioned features, the crystal

structures also revealed the presence of an unusual beta finger that is unique to the RNase H domain of Prp8 [6, 30]. At the junction where the N-terminal RNase H domain juxtaposes the C-terminal alpha helices, a ~25 Å channel is formed, which is likely a double-stranded RNA binding pocket [6] (**Fig. 5**). In fact, cross-linking experiments have shown that the Prp8 RNase H domain interacts with the 5' splice site [30].
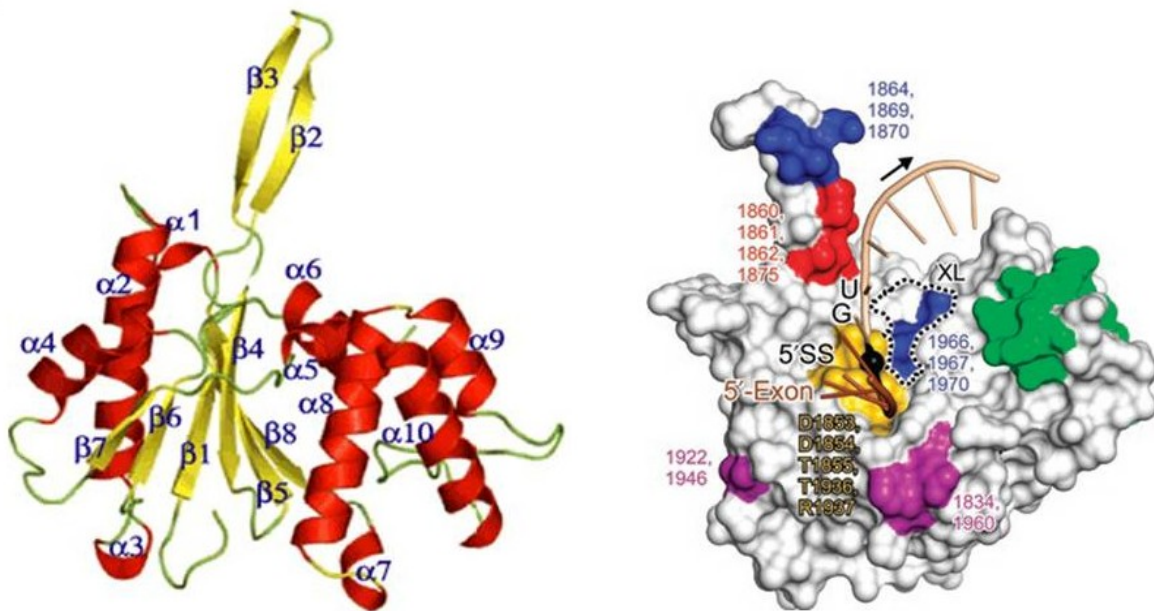
Figure 5: Human RNase H domain. Left: The ribbon structure of human Prp8_{1769-1990}. Alpha helices and beta sheets are shown in red and yellow respectively. Sequence contains two domains; the N-terminal RNase H domain and the C-terminal cluster of alpha helices. The β2-β3 represents the beta finger unique to Prp8 RNase H domain. Right: Space-filling model of the corresponding yeast Prp8 domain showing possible interaction with the 5' splice site of pre-mRNA.

RNase H is a metalloenzyme that generally uses two metal ions coordinated by four conserved carboxylates to specifically cleave RNA that hybridizes to DNA; however, the RNase H domain of Prp8 has only has two aspartate residues (D1853 and D1854 in yeast and D1782 and D1781 in human) at the positions corresponding to two of the four metal-coordinating carboxylates [6, 30]. Moreover, no bound metal ions were observed in either human or yeast crystal structures [30, 34]; however, D1853A and

D1854A mutants showed a temperature-sensitive phenotype [30]. Therefore, this observation, together with the fact that the conserved aspartate residues lie in close proximity to the 5' splice site, suggests that pre-mRNA catalysis may be carried out by two conserved aspartate residues and two metal-coordinating ligands in snRNA, making the catalytic components of the spliceosome a ribonucleoprotein. Alternatively, it is hypothesized that Prp8 is capable of bringing the catalytically important RNA components of the spliceosome together to facilitate the formation of the active-site conformation [24, 25], hence Prp8 is a protein cofactor for an RNA enzyme [32].
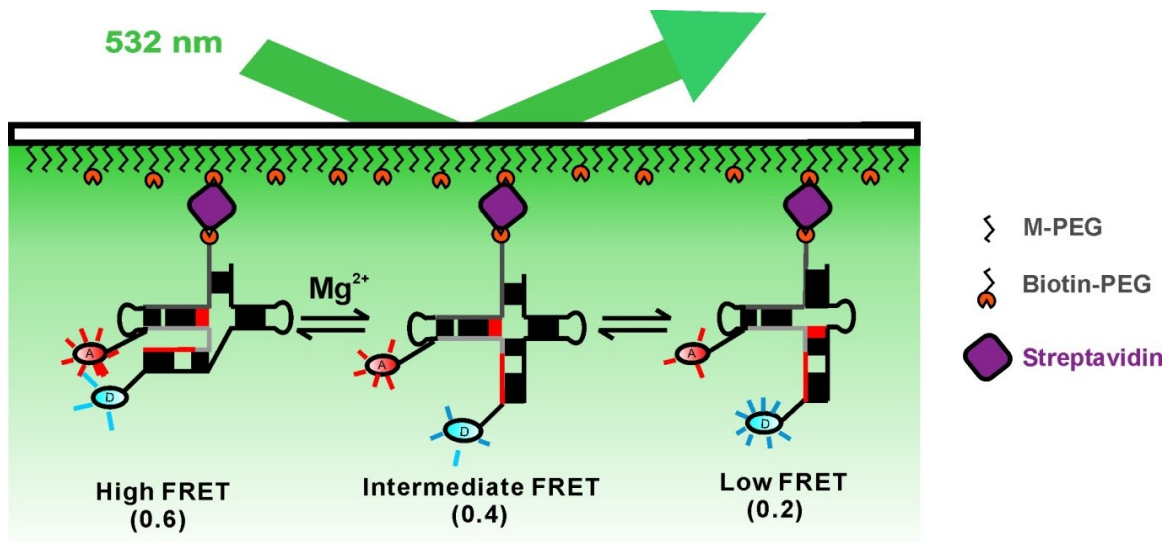
Figure 6: The smFRET experiment setup. U2-U6 is immobilized to a quartz slide via biotin-streptavidin link. The donor (Cy3) and the acceptor (Cy5) are attached to U6. The U2-U6 conformational changes are measured based on the change in FRET between the donor and the acceptor.

1.5: Splicing errors are attributed to many diseases. Errors in splicing are correlated with a number of diseases, including various forms of cancer such as leukemia and ovarian cancer, neurodegenerative disorders like Parkinson's disease, and genetic disorders like cystic fibrosis [35-39]. Therefore, understanding the detailed mechanism

and dynamics of the molecules involved in splicing is important to understand the underlying molecular mechanisms of related diseases.

1.6: Sm-FRET can be used to study U2-U6 dynamics. Single-molecule fluorescence resonance energy transfer (smFRET) is a versatile technique that allows studies of the dynamics of biological molecules that are otherwise hidden in ensemble-average experiments [40]. SmFRET involves labeling the molecules with at least two fluorophores; the donor and the acceptor fluorophores, and only the donor is excited with an appropriate wavelength laser. During smFRET studies, it is important to reduce background fluorescence, and for this purpose our lab uses prism-based total internal reflection fluorescence (TIRF) microscopy. In TIRF, the laser reaches the prism at an angle greater than the critical angle, at which the incident beam is totally internally reflected and does not penetrate into the sample [40]. Instead, an evanescent wave is generated at the slide-solution interface. The evanescent wave only penetrates a few hundred nanometers (100-300 nm) into the solution, which then excites only the molecules close to the slide surface, and therefore reduces the background fluorescence [40].

In our study, a minimal U6 construct is labeled with Cy3 (donor) and Cy5 (acceptor) fluorophores, and the donor is excited with a 532 nm laser (**Fig. 6**). Depending on the distance between the donor and the acceptor, some of the donor-emitted energy is transferred to the acceptor, due to the fact that the Cy3 emission spectrum overlaps with the Cy5 absorption spectrum. The efficiency of the energy transfer is given by

$$E = \frac{1}{1 + \left(\frac{R}{R_0}\right)^6}$$

where R is the distance between donor and acceptor, R_0 is the Förster distance, *i.e.* the distance that corresponds to 50% efficient energy transfer.

In our single-molecule FRET experiments, the intensities of the donor and the acceptor fluorophores are collected through the microscope objective and directed to a CCD camera in two separate channels. The apparent FRET value is given by

$$FRET = \frac{I_A}{(I_A + I_D)}$$

where I_A and I_D are the intensities of the acceptor and the donor, respectively. The variation of FRET over time then allows the determination of the relative distances between the donor and the acceptor, which in turn provides valuable information about the structural dynamics of individual molecules. FRET can therefore be regarded as a molecular ruler to study the conformational dynamics within biological systems.

CHAPTER 2: Materials and methods

2.1: RNA purification and labeling. RNA sequences (Table 1) were purchased from the Keck Foundation Resource Laboratory at the Yale University School of Medicine and purified and labeled as described [41, 42]. The 2'-hydroxyl protection groups were removed as described [41]. The RNAs were purified by denaturing gel electrophoresis (20% wt/vol polyacrylamide and 8 M urea) and diffusion eluted against elution buffer (0.5 M NH₄OAc and 0.1 mM EDTA) overnight at 4 °C, followed by chloroform extraction and ethanol precipitation. The U6 was labeled with Cy5 (GE Healthcare). The labeled RNA was precipitated by ethanol precipitation and purified by C8 column reverse-phase HPLC to remove unlabeled and non-deprotected RNA. RNA concentrations were measured by UV-Vis absorbance at 260 nm.

Name	Description	Sequence
U6	X = dT with C6 amino linker for Cy5 labeling	Cy3-AUACAGAGAUGAUCAGCAGUUCCCCXGCAUAAG GAUGAACCGUUUUACAAAGAGAU-Biotin
U6$_F$	X = Fluorescein	XAUACAGAGAUGAUCAGCAGUUCCCCXGCAUAAG GAUGAACCGUUUUACAAAGAGAU
U6-1	X = dT with C6 amino linker for Cy3 labeling	Cy5-AUACAGAGAUGAUCAGCAGUUCCCCX
U6-2	X = Δ/G/C/A Z = Biotin	AGGAXGAACCGUUUUACAAAGAGAUZ
U2		UAUGAUGUGAACUAGAUUCGGUUUUCCGUUUCUCUA

Table 1: RNA sequences used in the study. The symbol Δ denotes U80 deletion.

2.2: MALDI-MS Experiment. Matrix-assisted laser desorption ionization-mass spectrometry (MALDI-MS) was carried out for Cy3-U6 sample to confirm the position of the modified nucleotide and therefore the position of Cy5. The RNA sequence (300 pmol) was RNase T1 digested for 15 minutes to produce smaller fragments. The molecular weights of the fragments were calculated by using the Mongo Oligo Mass Calculator v2.06. After RNase T1 digestion, the reaction was quenched in dry-ice, dried and dissolved in 1 µL water. A saturated MALDI matrix solution was prepared by mixing 3-hydroxypicolinic acid (HPA) in 50% acetonitrile. The MALDI matrix (1 µL), 100 mM ammonium citrate (0.5 µL) and RNase T1 digested RNA sample (1 µL) were mixed on the MALDI plate in the given order. The spot was dried and used in MALDI experiment. A representative spectrum for Cy3-U6 is shown in Figure 7. The peak that appears at 2654.716 corresponds to the fragment with the amino-modified nucleotide used for Cy5 labeling. In addition to the fragment with the modified nucleotide, most of the other digested fragments were also observed within a reasonable error (**Table 2**).
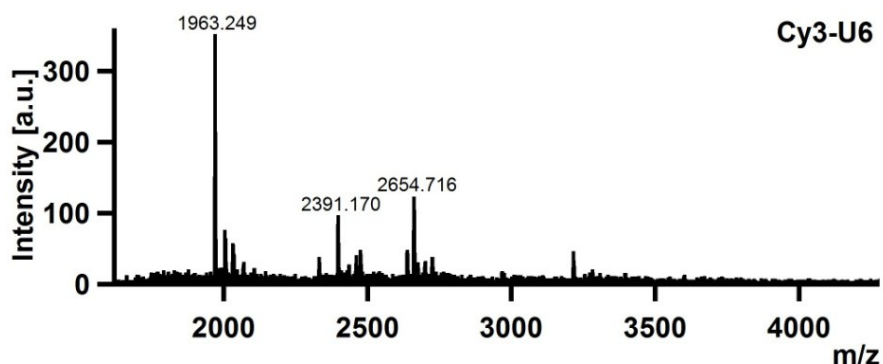

Figure 7: The MALDI result reveals the mass of the fragment that is used for Cy5 labeling. The peak that appears at 2654.716 is the mass of the fragment containing the modified nucleotide for Cy5 labeling. The peaks at 1963.249 and 2391.170 are two other resulting fragments after RNase T1 digestion.

Fragment	Sequence	Expected mass	Expected mass (without 3'-Phosphate)	Observed mass
A1:G6	pAUACAGp	3267.597	3249.579	N/O*
A7:G8	AGp	692.433	674.418	693.985
A9:G11	AUGp	998.602	980.587	999.348
A12:G16	AUCAGp	1632.995	1614.980	1633.940
C17:G19	CAGp	997.617	979.602	999.348
U20:G26	UUCCCCGp	2654.708	2636.693	2654.716
C27:G32	CAUAAGp	1962.204	1944.189	1964.155
G33:G33	Gp	363.224	345.209	N/O*
A34:G36	AUGp	998.602	980.587	999.348
A37:G41	AACCGp	1632.010	1613.995	1633.940
U42:G51	UUUUACAAAGp	3209.919	3191.904	3211.360
A52:G53	AGp	692.433	674.418	693.985
A54:U59	AUUUAU	2390.739		2391.170

Table 2: The expected and the observed masses from MALDI-MS experiments for the fragments resulted after RNase T1 digestion. All the masses are observed within a 0.5% error. * Not observed.

2.3: Protein purification. The plasmid pMAL-c2x (containing the amino acid sequence 1806-2413 of Prp8 with maltose binding protein (MBP) fused to the carboxyl terminus of Prp8 fragment) was obtained from McMillan's lab at the University of Alberta. The plasmid was inserted into a BL21 expression vector and expressed the cells at 22 °C to an optical density of 0.4-0.5, at which point the cells were induced by adding 0.3 μM IPTG, followed by overnight incubation. The culture was centrifuged, to collect the cell pellet. The cells were lysed by dissolving the pellet in the lysis buffer (20 mM Tris-Cl pH 8.0, 100 mM KCl, 5 mM BME). The supernatant containing proteins was obtained and passed through the amylose column. Prp8 binds to the amylose resin via MBP. The protein was then eluted with the elution buffer (20 mM Tris-Cl pH 8.0, 100 mM KCl, 5 mM BME, 10 mM maltose) and cleaved by the TEV protease to remove MBP. Anion-exchange column (Q-column) was used to separate MBP from Prp8. [30]. The SDS gel containing the purified Prp8 fragment is shown in the figure 8.
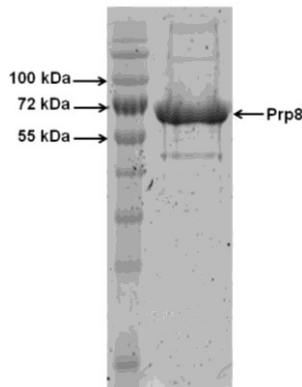
Figure 8: The 8% SDS gel for Prp8 purification. Left: EZ-Run, pre-stained protein ladder. Right: Prp8$_{1806-2413}$. The size of Prp8 Prp8$_{1806-2413}$ is 69 kDa.

2.4: Gel-shift assays. The two RNAs, U2 (4 µM) and U6 (2 µM), were annealed (50 mM Tris-Cl pH 7.5, 100 mM NaCl, 10 mM MgCl$_2$) by heating at 94 °C for 45 s, followed by 20 min incubation at room temperature. Prp8 was added and incubated for 30 min to allow it to interact with the U2-U6 complex. An equal volume of 40% glycerol was added to the reaction mixture and the samples were run on a native gel (8% acrylamide 40% w/v) using a 50 mM Tris-acetate pH 7.5, 10 mM magnesium acetate, 100 mM sodium acetate and 5 mM DTT buffer at 4 °C for 8 h at 100 V. The gel was fluorescence imaged using a Typhoon imager (GE Healthcare) by exciting the Cy3 donor fluorophore at 532 nm.

2.5: Fluorescence anisotropy experiments. Anisotropy experiments were carried out using a spectrofluorometer with automated polarizers (Varian, Carry Eclipse). The U6 RNA with 5' fluorescein (25 nM) and U2 RNA (50 nM) were mixed in a standard buffer (50 mM Tris-HCl pH 7.5, 100 mM NaCl, and 10 mM MgCl$_2$) and heated at 94 °C for 45 s and then annealed at room temperature for 20 min. Anisotropy was measured for Prp8 concentration from 0-60 µM. Fluorescein was excited at 490 nm (5 nm bandwidth),

parallel ($I_\parallel$) and perpendicular ($I_\perp$) emission intensities were measured at 520 nm (5 nm bandwidth). Fluorescence anisotropy (r) is given by

$$r = \frac{I_\parallel - GI_\perp}{(I_\parallel + 2GI_\perp)}$$

where G is an instrument-dependent correction factor.

2.6: Single-molecule experiments. The experimental setup shown in Figure 6 was used. Single-molecule FRET (smFRET) experiments were performed as described below. The U2 (4.0 µM) and U6 (2.0 µM) RNAs were annealed in standard buffer (50 mM Tris-HCl pH 7.5, 100 mM NaCl, and 10 mM $MgCl_2$ in saturating trolox) by heating a 10 µL solution at 94 °C for 45 s and cooling at room temperature for 20 min. The U2-U6 complex was diluted to 25 pM and immobilized onto a streptavidin-coated quartz slide via biotin to generate a surface density of ~0.1 molecules/µm^2. In order to prevent non-specific protein binding, the quartz slides were treated with polyethylene glycol (PEG) during slide preparation. The protein was injected along with an oxygen scavenging system (OSS) (10 nM Protocatechuic acid (PCA) and 2.5 mM Protocatechuate-3,4-dioxygenase (PCD) and standard buffer) and the slide was incubated for 30 min. The donor fluorophore was excited in a home-built total internal reflection microscope with a 532 nm laser (3 mW, Spectra-Physics Excelsior). The donor and the acceptor emissions were separated using appropriate dichroic mirrors (610DCXR, Chroma) and detected as two side-by-side images on a back-illuminated electron-multiplied CCD camera (Andor ixon).

CHAPTER 3: Results and discussion

Single-molecule experiments with U2 and U6 RNAs (Table 1) confirm previous data, that the U2-U6 complex adopts at least three FRET states, of which ~0.2 and ~0.4 are well populated while the ~0.6 state is only transiently populated at 10 mM Mg^{2+} concentration (**Fig. 9**). Previous SM data showed that increasing Mg^{2+} stabilizes the low
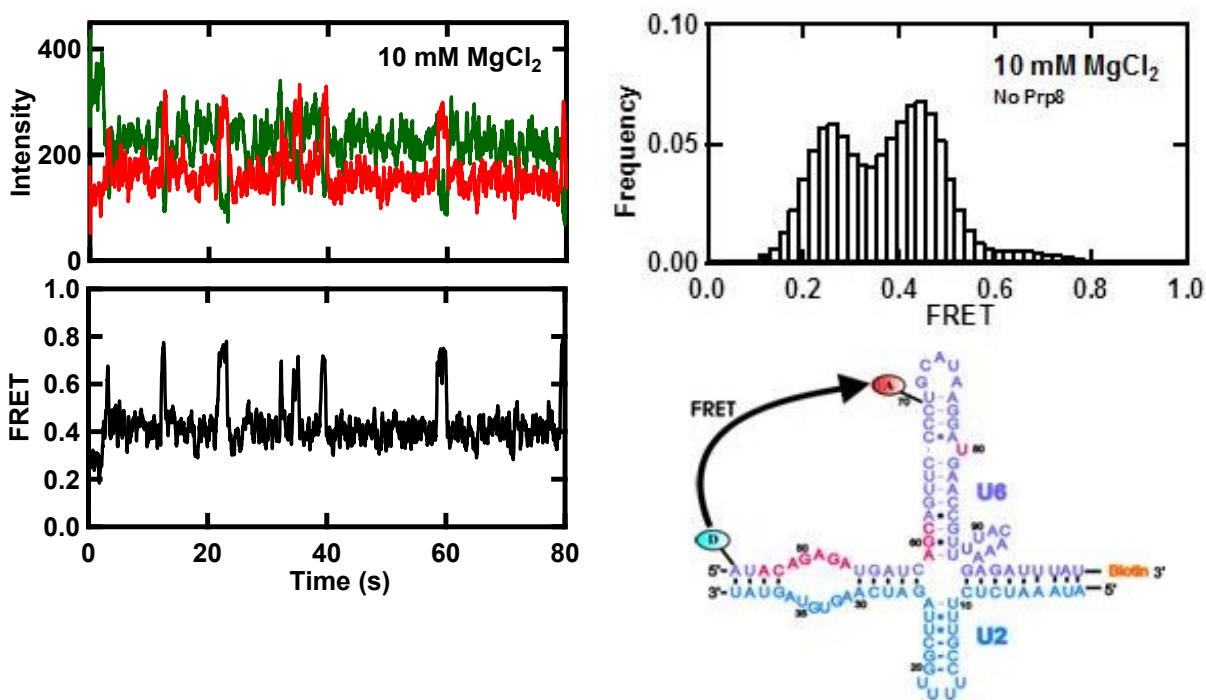
Figure 9: U2-U6 dynamics in the absence of Prp8. Left: Intensity (top) and the corresponding FRET trajectory (bottom) of a single U2-U6 complex showing all three FRET states. Donor and acceptor intensities are shown in green and red, respectively. Top right: The FRET histogram drawn with more than one-hundred molecules. At 10 mM Mg^{2+} 0.4 and 0.2 FRET states are mostly populated while 0.6 FRET state is only transiently populated. Bottom right: U2-U6 construct used in the study.

FRET states, thereby separating the U6 ISL from the ACAGAGA sequence; however, if the metal ion bound at the position U80 of U6 has a role in catalysis or related function, one would expect the opposite, *i.e.,* upon Mg^{2+} binding, U6 ISL comes closer to the ACAGAGA sequence and therefore increase the high FRET state. Many groups

therefore suggest that *in vivo*, proteins may be involved in stabilizing the favorable conformations important for efficient splicing. Since the RNase H domain of Prp8 protein interacts with catalytically important snRNAs and the pre-mRNA, we propose that Prp8 may be involved in the high FRET state stabilization. To study the effect of Prp8 on U2-U6 conformations, smFRET experiments were carried out in the presence of yeast Prp8$_{1806-2413}$ expressing both the RNase H and MPN domains.

3.1: Prp8$_{1806-2413}$ binds our U2-U6 complex. Gel-shift assays from the McMillan lab showed that the RNase H domain of human Prp8 binds to an RNA sequence that forms a four-helix junction similar to U2, U6 and the 5' splice site interaction of the spliceosome [30]. In order to test whether yeast Prp8$_{1806-2413}$ binds our U2-U6 construct, gel-mobility-shift assays and anisotropy experiments were carried out. Even though the binding affinity is low (~5% when Prp8 is 70 µM), the gel picture shows clearly that Prp8$_{1806-2413}$ binds our U2-U6 construct (Fig. 10). Compared to the unbound U2-U6, the bound U2-U6 complex has high FRET, indicating that Prp8 might be involved in stabilizing the high FRET state as we had hypothesized. The poor binding in the gel might result from instability of the U2-U6/ Prp8$_{1806-2413}$ complex in the gel. Therefore alternative methods were used to measure the binding affinity.

3.2: Fluorescence anisotropy measurements reveal Prp8$_{1806-2413}$ binding to U2-U6 complex. Fluorescence anisotropy can be used to monitor protein-nucleic acid interaction when one of the components is labeled with a fluorophore [43]. Anisotropy measurements compare the orientation of fluorophores between absorption and emission by monitoring emission intensity parallel and perpendicular to excitation. If a fluorophore attached to the molecule of interest interacts with a large molecule such as
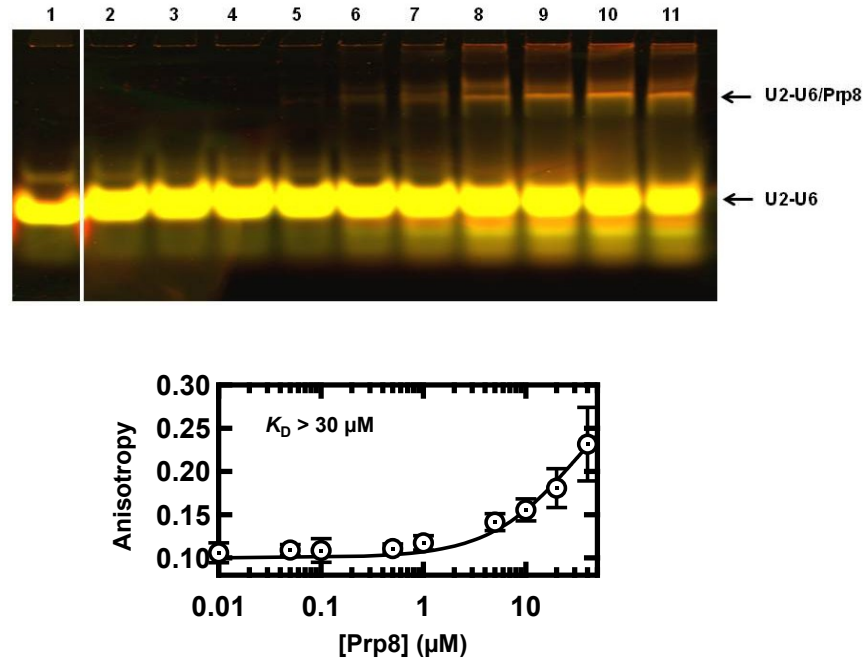
Figure 10: Prp8 weakly binds U2-U6. Top: Gel-mobility-shift assay with Prp8$_{1806-2413}$ and U2-U6 complex. Lane 1: U6, Lane 2: U2-U6 complex, Lane 3-11: U2-U6 complex and Prp8 (0.01, 0.1, 1, 5, 10, 20, 40, 60, 70 µM respectively). Bottom: Fitting the anisotropy values against Prp8 concentration to a quadratic equation gives a K_D value of ≥30 µM.

a protein, the rate of fluorophore tumbling decreases, and hence the anisotropy increases. In our study, we tested the change in anisotropy for a fluorescein-labeled U2-U6 complex with increasing Prp8 concentration. Supporting our native gel data, the results show that the anisotropy is increased with Prp8 concentration (**Fig. 10**). An estimated dissociation constant (K_D) of ≥30 µM was obtained by fitting the data to the quadratic equation,

$$f(Prp8) = r_0 + (r_{max} - r_0)\left[\frac{K_D + [RNA_0] + [Prp8] - \sqrt{(K_D + [RNA_0] + [Prp8])^2 - 4[RNA_0][Prp8]}}{(2 * RNA_0)}\right]$$

where r_0, r_{max}, RNA_0, and K_D are the lowest anisotropy value, highest anisotropy value, RNA concentration, and dissociation constant, respectively. We were not able to reach saturation in these experiments because we are limited by the concentration of the

protein stock. Compared to the gel-shift assays, anisotropy experiments reveal more Prp8 binding to U2-U6, supporting the idea that the U2-U6/Prp8 interaction is not stable during gel-shift assays.

3.3: Single-molecule studies reveal Prp8$_{1806\text{-}2413}$ stabilizes the high FRET states. Supporting our hypothesis, that Prp8$_{1806\text{-}2413}$ is involved in stabilizing the high FRET conformation, we observed a higher percentage of static and dynamic molecules at ≥0.6 FRET state (Fig. 11). Interestingly with increasing Prp8 concentrations, molecules with FRET states ~0.8 and ~1.0 were also observed (Fig. 10). Three FRET histograms
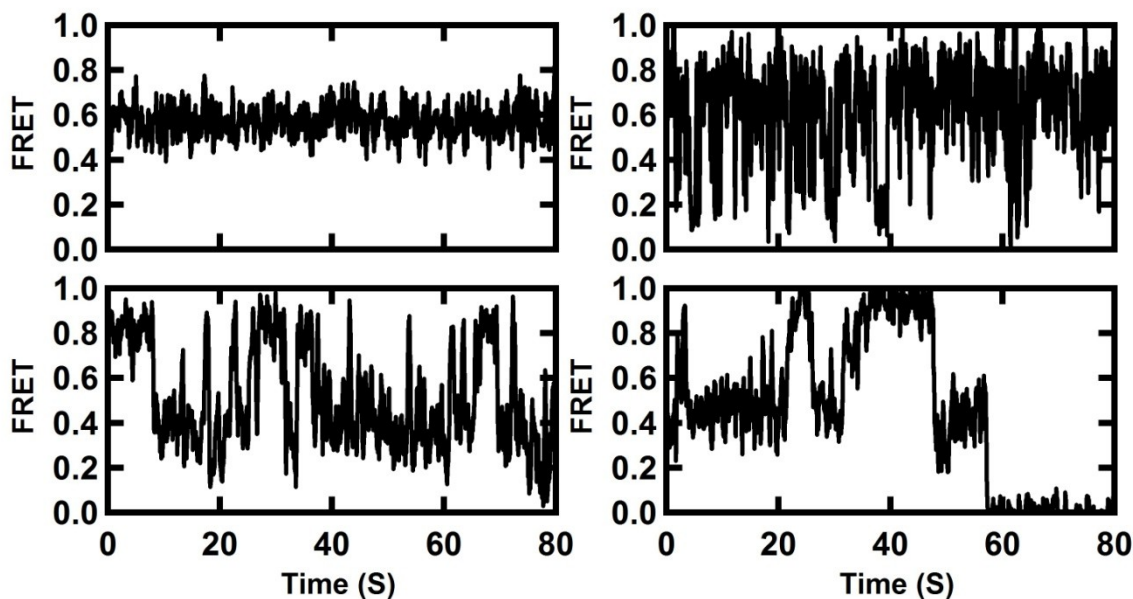
Figure 11: Characteristic molecules at ≥0.6 FRET states at 10 mM Prp8 concentration. Top left: static molecules at 0.6 FRET state, top right: fast dynamics between ~0.6 and ~0.2 FRET states, bottom left: dynamics between ~0.4 and ≥0.6 FRET states, bottom right: dynamics between ~0.4 and ~1.0 FRET states.

drawn from the smFRET experiments in the presence of Prp8 (0.001, 1 and 20 µM) are shown in Figure 12. From the histograms, it is clear that Prp8 increases the high FRET population compared to the low and intermediate FRET states. The fraction of ≥0.6
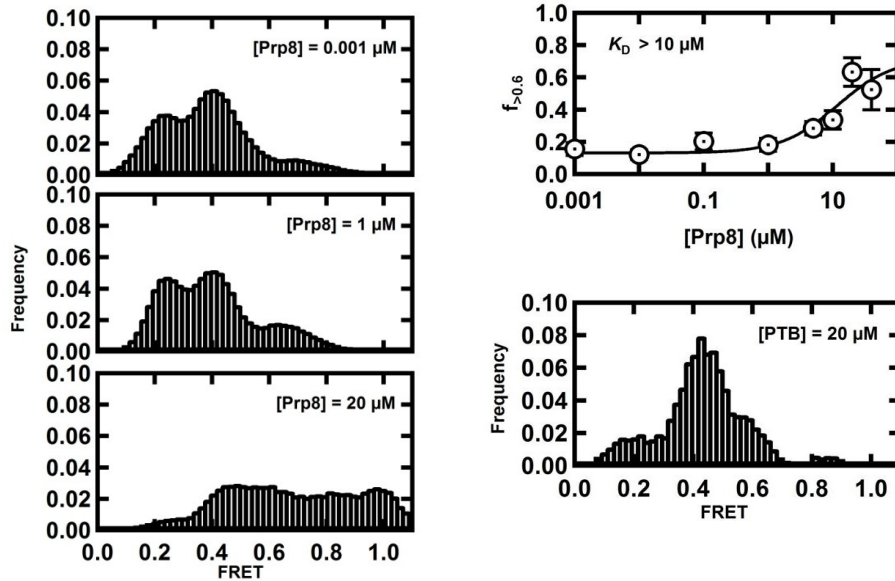
Figure 12: Prp8 stabilizes the high FRET states of U2-U6. Left: Higher Prp8 concentrations result a broad peak that extends from FRET 0.6-1.0. This may be because Prp8 brings the U6 ISL close to the ACAGAGA sequence and therefore Cy3 and Cy5 come very close together and most of the energy is transferred from the donor to the acceptor. The broad peak may result due to the fast dynamics at high Prp8 concentration. Top right: Fitting the fraction of molecules with ≥0.6 FRET state against Prp8 concentration to a modified Hill equation gives a K_D value of ≥10 µM. Bottom right: Control SM experiment with PTB at 20 µM concentration.

FRET states was calculated by integrating the histograms and values were plotted against Prp8 concentration (**Fig. 12**). Although we do not reach saturation, it is clear that with increasing Prp8 concentration, the ≥0.6 FRET state is increased. A dissociation constant of ≥10 µM was estimated by fitting the data to a modified Hill equation,

$$ f(x) = f_0 + (f_{max} - f_0)(\frac{x^\wedge n}{K_D^{\wedge} n + x^{\wedge} n}) $$

where f_0, f_{max}, n, X and K_D are the initial fraction of molecules with ≥0.6 FRET state, the final fraction of molecules with ≥0.6 FRET state, the Hill coefficient, Prp8 concentration, and the dissociation constant, respectively. The estimated K_D is comparable with a

dissociation constant from a previous study for a closely related Prp8 domain and RNA sequence [30]. In order to test the specificity of Prp8 in stabilizing the high FRET states, a control experiment was carried out with the protein PTB (Polypyrimidine Tract Binding) at 20 µM concentration. The corresponding histogram shows (**Fig. 12**) that the high FRET states were not increased with PTB indicating that Prp8 specifically increases the high FRET states of U2-U6 complex.
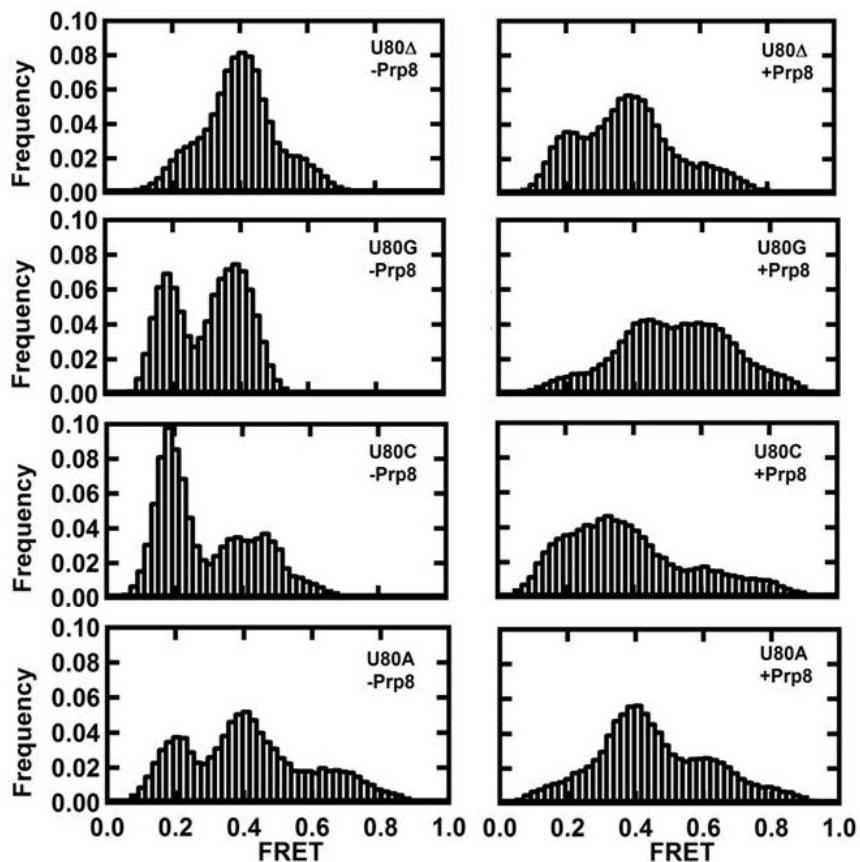
Figure 13: Experiments with U6 which are mutated/deleted at the position U80 in the presence of Prp8. The high FRET states are considerably rescued when the U80 is replaced to a different nucleotide than when it is deleted.

3.4: Prp8 stabilizes the high FRET states of the U80 mutants. Previous studies from our lab showed that the U2-U6 complex forms three base-triple interactions (G86-C61·U80, U87-G60·G52 and U88-A59·A53) that are important in the stabilization of the

high FRET state [25] (**Fig. 4**). In order to investigate the contribution of these base triples and Prp8, separately on the stabilization of the high FRET state, single-molecule experiments were carried out using U80 mutated U6 sequences in the presence and absence of Prp8 (20 µM) (**Fig. 13**). A three-piece U2-U6 constructs were used in the study (The GCAUA penta-loop was deleted from the minimal U6 in Figure 8 and therefore U6 comes in two pieces).

The high FRET stabilization is more apparent when U80 is replaced with G/C/A than when it is deleted. This may indicate that the high FRET states stabilization by Prp8 mainly depends on the presence of a nucleotide rather than its identity at the U80 position. Our results show that Prp8 considerably stabilizes high FRET states of U80G. However, previous studies have shown that U80G has a lethal phenotype [21]. Therefore we hypothesized that not only the high FRET conformation, but also the identity of the nucleotide is important for the splicing activity. These nucleotides might have crucial functions such as metal ion binding and/or structural effect.

In summary, the RNase H domain of Prp8 interacts with the minimal U2-U6 construct weakly and it is involved in stabilizing the high FRET state. Furthermore, in addition to the ~0.6 high FRET state that is observed at 10 mM $MgCl_2$ in a protein-free environment, at high Prp8 concentration, a broad band that extends from FRET 0.6-1.0 was reported (**Fig. 12**). This may due to the fact that Prp8 brings the U6 ISL close in proximity to the ACAGAGA sequence and AGC triad (**Fig. 14**) and therefore most of the energy is transferred from the donor to the acceptor.
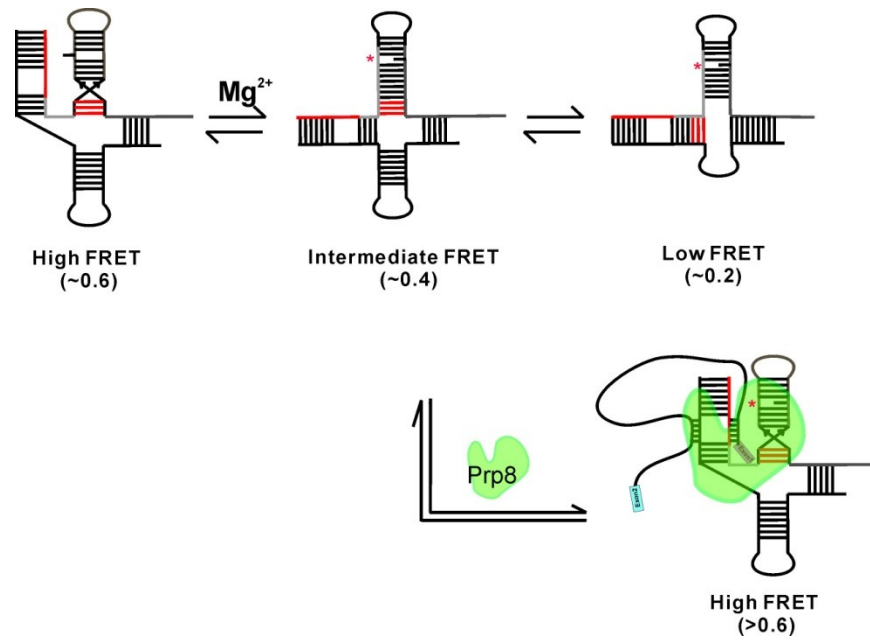
Figure 14: The proposed model for Prp8 in the vicinity of U2-U6. In the presence of Mg^{2+}, U2-U6 favors the low FRET states and therefore the high FRET states and transiently populated. However, in the presence of Prp8, at the same Mg+ concentrations, the high FRET states are dominated.

CONCLUSIONS

We have carried out sm-FRET experiments to study the effect of Prp8 on the conformational dynamics of a minimal U2-U6 construct. In the absence of Prp8, low and intermediate U2-U6 FRET states are more populated while the high FRET states are only transiently sampled. In the presence of Prp8, however, the high FRET states are dominant. A broad band that extends from 0.4-1.0 results at high Prp8 concentration, possibly because Prp8 transiently interacts and partially unwinds helix III resulting in faster dynamics. Moreover, the results with the U6 mutants show that Prp8 can at least partially rescue the high FRET states of U80A, U80G and U80C, while it has only a minimal effect on U80Δ. Therefore, we suggest that the presence of a nucleotide, rather than its identity is important in stabilizing the high FRET states by Prp8 and hence the action of Prp8 is robust. As U80G is lethal [21], we suggest that in addition to the high FRET states, the identity of the nucleotide is important for the activity. Overall, based on our results we propose a model for the action of the RNase H domain of Prp8 in the vicinity of U2-U6 (**Fig. 14**). The increase in time spent in the high FRET states in the presence of Prp8 suggests that Prp8 may assist in bringing the U6 ISL in close proximity to the U6 ACAGAGA sequence, and therefore, placing the catalytically important metal ion at U80 close to the 5' splice site.

Overall, results in this study enable us to understand the dynamics of the U2-U6 complex at the catalytic center of the spliceosome. The study is exciting as the results from this thesis may lead towards the discovery of novel therapeutics to cure human diseases that arise from splicing errors.

CHAPTER 4: Future directions

Our data suggest that Prp8 stabilizes the U2-U6 high FRET conformations. In order to further investigate the role of Prp8 in modulating the U2-U6 conformations, we propose to perform smFRET experiments using mutant Prp8 and U2-U6. The beta-finger of the RNase H of Prp8 contains both the first- and second- step alleles [33]. It is hypothesized that the first-step complex is stabilized by the first-step alleles, while it is destabilized by the second-step alleles [33]. We propose to carry out smFRET experiments with the first- and second-step alleles of Prp8 (**Fig. 15**) to study their effects on U2-U6 dynamics. We expect to observe different U2-U6 dynamics for different alleles, in particular, more high FRET state for the first-step alleles than for the second-step alleles.
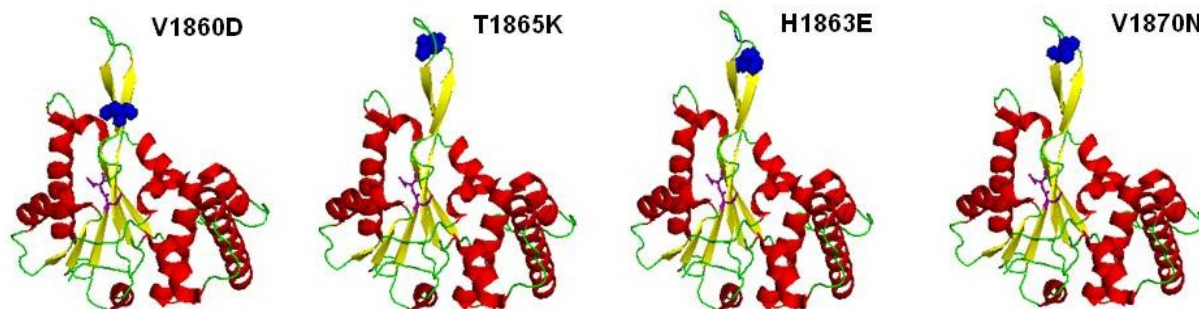
Figure 15: The first- (V1860D and T1865K) and second-step (H1863E and V1870N) alleles of Prp8. Shown in purple are D1853 and D1854 which form an incomplete active site.

The D1854 is one of the aspartate residues that form an incomplete active site of the RNase H domain of Prp8 and the D1854A mutation has a temperature sensitive phenotype (**Fig. 15**). We propose to perform single-molecule experiments with Prp8-D1854A to test the effect of the mutation on U2-U6 dynamics. With the mutant Prp8, we

expect to observe U2-U6 dynamics that are different from the U2-U6 dynamics in the presence of the wild-type Prp8.
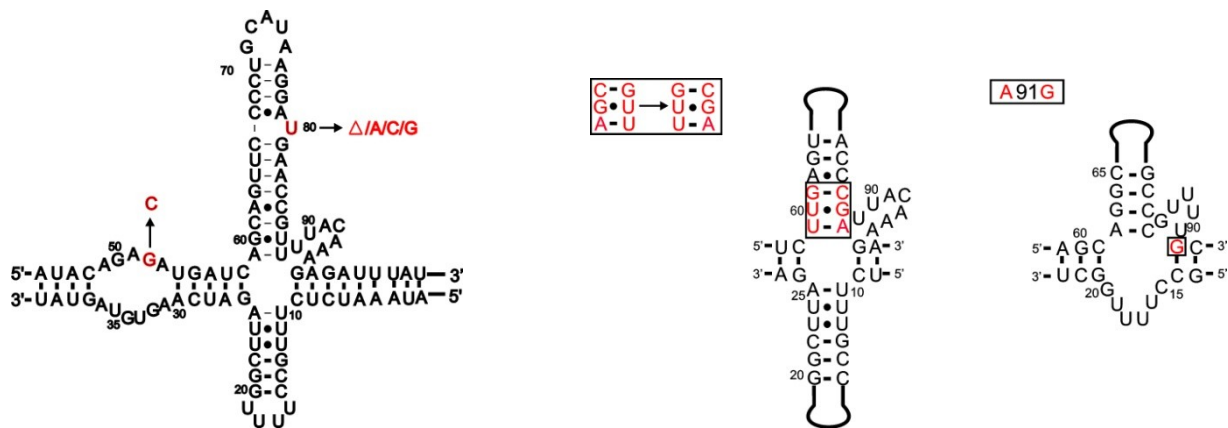
Figure 16: The proposed mutants for U2-U6. Left: The minimal U6 showing the mutations at U80 and G52. Left: The six-fold U6 mutant that favors the formation of four-helix junction and the A91G mutation of U6 that favors the formation of the three-helix junction.

We propose to carry out smFRET experiments with a G52C U6 mutant that disrupts the U87-G60·G52 base triple (**Fig. 16**). In the absence of Prp8, the G52C mutation eliminates the high FRET state. It is also important to note that G52 is protected from RNase T1 and RNase A digestion in the presence of saturating concentration of the RNase H domain of human Prp8, indicating that Prp8 interacts with G52 [30].

A six-fold mutant (**Fig. 16**) of U6 that prevents the formation of helix IB while maintaining the stability of the U6 ISL has previously shown that molecules mostly exist in the ~0.4 FRET state and occasionally go to the ~0.6 FRET state [25]. On the other hand, the U6 A91G mutation (**Fig. 16**) favors the formation of helix IB by extending helix II and thereby stabilizing it relative to the U2 stem I [25]. Therefore, this six-fold mutant U6 (the last three base pairs of the extended U6 ISL are swapped) and A91G U6 will be

used in our study to test the ability of Prp8 to increase the high FRET population when the U2-U6 complex preferentially exists either in the ~0.2 or ~0.4 FRET state.

We will also use the RNase H domain of human Prp8 to study the effect of the protein on the human U2-U6 complex, and hence, compare the effects of the RNase H domain of human and yeast Prp8 on the U2-U6 dynamics. Altogether the results from this study will explain the role of RNase H domain of both human and yeast Prp8 in stabilizing U2-U6 conformations during splicing catalysis.

REFERENCES

1. Will, C.L. and R. Luhrmann, *Spliceosome structure and function.* Cold Spring Harbor perspectives in biology, 2011. **3**(7).

2. Hoskins, A.A. and M.J. Moore, *The spliceosome: a flexible, reversible macromolecular machine.* Trends in biochemical sciences, 2012. **37**(5): p. 179-88.

3. Sontheimer, E.J., *The spliceosome shows its metal.* Nature structural biology, 2001. **8**(1): p. 11-3.

4. Nilsen, T.W., *The spliceosome: the most complex macromolecular machine in the cell?* BioEssays : news and reviews in molecular, cellular and developmental biology, 2003. **25**(12): p. 1147-9.

5. Valadkhan, S. and J.L. Manley, *Intrinsic metal binding by a spliceosomal RNA.* Nature structural biology, 2002. **9**(7): p. 498-9.

6. Abelson, J., *Is the spliceosome a ribonucleoprotein enzyme?* Nature structural & molecular biology, 2008. **15**(12): p. 1235-7.

7. Villa, T., J.A. Pleiss, and C. Guthrie, *Spliceosomal snRNAs: Mg(2+)-dependent chemistry at the catalytic core?* Cell, 2002. **109**(2): p. 149-52.

8. Grainger, R.J. and J.D. Beggs, *Prp8 protein: at the heart of the spliceosome.* RNA, 2005. **11**(5): p. 533-57.

9. Madhani, H.D. and C. Guthrie, *A novel base-pairing interaction between U2 and U6 snRNAs suggests a mechanism for the catalytic activation of the spliceosome.* Cell, 1992. **71**(5): p. 803-17.

10. Sashital, D.G., et al., *U2-U6 RNA folding reveals a group II intron-like domain and a four-helix junction.* Nature structural & molecular biology, 2004. **11**(12): p. 1237-42.

11. Seetharaman, M., et al., *Structure of a self-splicing group II intron catalytic effector domain 5: parallels with spliceosomal U6 RNA.* RNA, 2006. **12**(2): p. 235-47.

12. Martinez-Abarca, F. and N. Toro, *Group II introns in the bacterial world.* Molecular microbiology, 2000. **38**(5): p. 917-26.

13. Jacquier, A., *Group II introns: elaborate ribozymes.* Biochimie, 1996. **78**(6): p. 474-87.

14. Hilliker, A.K. and J.P. Staley, *Multiple functions for the invariant AGC triad of U6 snRNA.* RNA, 2004. **10**(6): p. 921-8.

15. Mefford, M.A. and J.P. Staley, *Evidence that U2/U6 helix I promotes both catalytic steps of pre-mRNA splicing and rearranges in between these steps.* RNA, 2009. **15**(7): p. 1386-97.

16. Costa, M. and F. Michel, *Frequent use of the same tertiary motif by self-folding RNAs.* The EMBO journal, 1995. **14**(6): p. 1276-85.

17. Fabrizio, P. and J. Abelson, *Thiophosphates in yeast U6 snRNA specifically affect pre-mRNA splicing in vitro.* Nucleic acids research, 1992. **20**(14): p. 3659-64.

18. Reiter, N.J., et al., *Structure of the U6 RNA intramolecular stem-loop harboring an S(P)-phosphorothioate modification.* RNA, 2003. **9**(5): p. 533-42.

19. Yean, S.L., et al., *Metal-ion coordination by U6 small nuclear RNA contributes to catalysis in the spliceosome.* Nature, 2000. **408**(6814): p. 881-4.

20. Toor, N., et al., *Crystal structure of a self-spliced group II intron.* Science, 2008. **320**(5872): p. 77-82.

21. Sashital, D.G., et al., *Structural basis for a lethal mutation in U6 RNA.* Biochemistry, 2003. **42**(6): p. 1470-7.

22. Valadkhan, S., *Role of the snRNAs in spliceosomal active site.* RNA biology, 2010. **7**(3): p. 345-53.

23. Sun, J.S. and J.L. Manley, *A novel U2-U6 snRNA structure is necessary for mammalian mRNA splicing.* Genes & development, 1995. **9**(7): p. 843-54.

24. Burke, J.E., et al., *Structure of the yeast U2/U6 snRNA complex.* RNA, 2012. **18**(4): p. 673-83.

25. Guo, Z., K.S. Karunatilaka, and D. Rueda, *Single-molecule analysis of protein-free U2-U6 snRNAs.* Nature structural & molecular biology, 2009. **16**(11): p. 1154-9.

26. Guo, Z., *Single molecule studies of spliceosomal snRNAs U2-U6*, in *Chemistry*2010, Wayne State University: Detroit.

27. Pena, V., et al., *Structure and function of an RNase H domain at the heart of the spliceosome.* The EMBO journal, 2008. **27**(21): p. 2929-40.

28. Valadkhan, S. and Y. Jaladat, *The spliceosomal proteome: at the heart of the largest cellular ribonucleoprotein machine.* Proteomics, 2010. **10**(22): p. 4128-41.

29. Dlakic, M. and A. Mushegian, *Prp8, the pivotal protein of the spliceosomal catalytic center, evolved from a retroelement-encoded reverse transcriptase.* RNA, 2011. **17**(5): p. 799-808.

30. Ritchie, D.B., et al., *Structural elucidation of a PRP8 core domain from the heart of the spliceosome.* Nature structural & molecular biology, 2008. **15**(11): p. 1199-205.

31. Valadkhan, S., *The spliceosome: caught in a web of shifting interactions.* Current opinion in structural biology, 2007. **17**(3): p. 310-5.

32. Collins, C.A. and C. Guthrie, *The question remains: is the spliceosome a ribozyme?* Nature structural biology, 2000. **7**(10): p. 850-4.

33. Yang, S., et al., *A multi-center open-labeled study of recombinant erythropoietin-beta in the treatment of anemic patients with multiple myeloma, low-grade non-Hodgkin's lymphoma, or chronic lymphocytic leukemia in Chinese population.* International journal of hematology, 2008. **88**(2): p. 139-44.

34. Yang, K., et al., *Crystal structure of the beta-finger domain of Prp8 reveals analogy to ribosomal proteins.* Proceedings of the National Academy of Sciences of the United States of America, 2008. **105**(37): p. 13817-22.

35. Ward, A.J. and T.A. Cooper, *The pathobiology of splicing.* The Journal of pathology, 2010. **220**(2): p. 152-63.

36. Kalnina, Z., et al., *Alterations of pre-mRNA splicing in cancer.* Genes, chromosomes & cancer, 2005. **42**(4): p. 342-57.

37. Licatalosi, D.D. and R.B. Darnell, *Splicing regulation in neurologic disease.* Neuron, 2006. **52**(1): p. 93-101.

38.   Mills, J.D. and M. Janitz, *Alternative splicing of mRNA in the molecular pathology of neurodegenerative diseases.* Neurobiology of aging, 2012. **33**(5): p. 1012 e11-24.

39.   Ramalho, A.S., et al., *Transcript analysis of the cystic fibrosis splicing mutation 1525-1G>A shows use of multiple alternative splicing sites and suggests a putative role of exonic splicing enhancers.* Journal of medical genetics, 2003. **40**(7): p. e88.

40.   Zhao, R. and D. Rueda, *RNA folding dynamics by single-molecule fluorescence resonance energy transfer.* Methods, 2009. **49**(2): p. 112-7.

41.   Rueda, D. and N.G. Walter, *Fluorescent energy transfer readout of an aptazyme-based biosensor.* Methods in molecular biology, 2006. **335**: p. 289-310.

42.   Roy, R., S. Hohng, and T. Ha, *A practical guide to single-molecule FRET.* Nature methods, 2008. **5**(6): p. 507-16.

43.   LeTilly, V. and C.A. Royer, *Fluorescence anisotropy assays implicate protein-protein interactions in regulating trp repressor DNA binding.* Biochemistry, 1993. **32**(30): p. 7753-8.

ABSTRACT

THE SPLICEOSOMAL PROTEIN PRP8 STABILIZES A COMPACT CONFORMATION OF THE U2-U6 COMPLEX

by

S. A. L. IMALI SUBASINGHE

December 2012

Advisor: Prof. David Rueda

Major: Chemistry (Biochemistry)

Degree: Master of Science

The spliceosome is a large, RNA-protein complex that catalyzes pre-mRNA splicing during mRNA maturation. The RNA components (small nuclear RNA; snRNAs) of the spliceosome have been well studied and are believed to be involved in the splicing catalysis. Although proteins are essential for splicing, they may not be directly involved in catalysis. Among hundreds of proteins, Prp8 is the only protein that interacts with all of the catalytically important snRNAs. Therefore, it is hypothesized that Prp8 may catalyze splicing either by directly participating in catalysis or by stabilizing the conformation of the catalytically active spliceosome. In order to test whether or not Prp8 stabilizes the active-site conformation, we carried out single-molecule fluorescence resonance energy transfer (smFRET) experiments with catalytically important snRNAs U2 and U6 and Prp8. We observed that in the presence of Prp8, the population of the high FRET conformation of U2-U6 that is thought to be the active conformation increased indicating that one of the functions of Prp8 would be to stabilize the active site conformation of the spliceosome.

AUTOBIOGRAPHICAL STATEMENT

Name: S. A. L. IMALI SUBASINGHE

Education: **MS -** Chemistry - Major in Biochemistry

Wayne State University, Detroit, Michigan, USA

BS - Biochemistry and Molecular Biology,

University of Colombo, Colombo, Sri Lanka

Poster Presentations:

1. *The spliceosomal protein Prp8 stabilizes a compact conformation of the U2-U6 complex.* Chemistry Symposium, Wayne State University, Detroit, MI (October, 2012).

2. *The spliceosomal protein Prp8 stabilizes a compact conformation of the U2-U6 complex.* Rustbelt RNA Meeting, Dayton, OH (October, 2012).